A Coupling Experiment of an Atmosphere and an Ocean Model with a Monthly Anomaly Exchange Scheme

Liu Hui (刘　辉), *Jin Xiangze* (金向泽), *Zhang Xuehong* (张学洪)
and *Wu Guoxiong* (吴国雄)

Institute of Atmospheric Physics, Chinese Academy of Sciences, Beijing 100080

Received May 26, 1995; revised September 11, 1995

ABSTRACT

A nine−layer spectral atmospheric general circulation model is coupled to a twenty−layer global oceanic general circulation model with the "prediction−correction" monthly anomaly exchange scheme which has been proposed at the Institute of Atmospheric Physics (IAP). A forty−year integration of the coupled model shows that the CGCM is fairly successful in keeping a reasonable pattern of the modelled SST although most of the Pacific become warmer than those given by the uncoupled ocean model. The model tends to reach a more realistic state than the uncoupled one in terms of downward surface heat flux into ocean particularly in the equatorial Pacific region. Also, the model is capable to simulate interannual variability of sea surface temperature in tropical region.

Key words: Coupling experiment, Downward heat flux, Interannual variability

I. INTRODUCTION

Up to now, an increasing number of coupled atmosphere—ocean models has been developed all over the world to investigate interactions between the ocean and the atmosphere, especially the El Nino / Southern Oscillation and climate variability's with time scales of decade or even longer. However, these models are still in their early developing stage because almost all of them suffer from serious problems, for example, the "climate drifting" from their uncoupled mean states to very unrealistic states despite of their differences in physics, numerical and horizontal / vertical resolutions (Neelin et al., 1992).

At the Institute of Atmospheric Physics (IAP), a coupled GCM of low vertical resolution (two−layer AGCM and four−layer OGCM) was developed in 1992 (Zhang et al., 1992). A group of experiments on coupling scheme have been done with it and a "prediction−correction" monthly mean anomaly coupling scheme has been proposed and proved to be successful in controlling the climate drifting in the coupled model. This model also simulates realistic interannual SST variance in the equatorial Pacific region.

However, development of a higher vertical resolution CGCM seems to be necessary, because higher vertical resolution atmosphere and ocean models can give better simulation of short and long wave radiations within the atmosphere, surface exchange of momentum, sensible and latent heat within surface boundary layer between the atmosphere and the ocean, as well as thermohaline circulation in the ocean. A 9−layer spectral AGCM (L9R15) and a 20−layer OGCM are available at IAP in 1994. Since that time, an attempt has been devoted to develop a coupled model based on the 9−layer spectral AGCM and the 20−layer OGCM. A coupling experiment with these two models has been completed recently. The coupled GCM has been integrated for 40 years and has shown only a little climate drifting and reasonable interannual SST variability in equatorial region. This coupled model and it's

preliminary performance will be described in this paper.

A brief description of the atmospheric and oceanic components of the CGCM, as well as the coupling scheme are given in Section 2. An analysis of the climate drifting by means of the diagnoses of SST and sea–level air pressure (SLP), as well as heat flux into ocean are shown in Sections 3 and 4 respectively. Section 5 shows the modelled interannual variability of SST in the equatorial region. Summary and discussion are given in Section 6.

II. THE MODEL

The atmospheric portion of the CGCM is a nine–layer spectral (R15) AGCM in σ–coordinate (Wu et al., 1996). It consists of a special dynamical framework, in which departures of temperature and geopotential from a stratified reference atmosphere are used as the model's variables (Zeng, 1979; Chen, 1987). In the model, a global mean stratification of temperature $\overline{T}(p)$, defined by formula:

$$C_0^2 = \frac{R^2\,\overline{T}(p)}{g}\left(\frac{g}{C_p} + \frac{\partial\overline{T}(p)}{\partial z}\right) = \text{constant}$$

is used as the reference stratification. This greatly decreases the errors due to the spectral truncation of real topography in the model. The radiation absorbers in the model include cloud, water vapour. CO_2 and O_3. The high–, middle–, and low–level cloud are considered but not as prognostic variables. Cloud amounts and heights are prescribed in terms of the observed values, which are zonally meant and monthly averaged. The model's convection is performed by dry / moist convective adjustment scheme (Manabe et al., 1965) and is independent on the clouds. The surface drag coefficient is dependent on hydrostatic stability, and the gustiness parameter is set to 1.0 m / s. The runoff into ocean is not included in the current model. Snow cover over land is prescribed climatologically. The model has been integrated for 14 years with the AMIP climatological monthly mean SST and sea ice[①]forcing which is interpolated to each day and does not have interannual variation. It reproduces satisfactorily many aspects of the contemporary mean climate, especially the earth surface mean climate.

The oceanic portion is the recently developed IAP twenty–layer OGCM (Zhang et al., 1994). It is a grid model with resolution of 4° latitude by 5° longitude. The model is a fully primitive equation model with free surface rather than using rigid–lid approximation. The zonal mean stratification of temperature. salinity (from Levitus, 1982) as well as density and pressure are introduced into the model's governing equations. Therefore, all thermodynamic variables are replaced by their departures from the stratifications. The model's geography is fairly realistic except that the Arctic sea is not included and the northern boundary of the North Atlantic is closed at 72°N. The bottom topography of the model is also realistic with a maximum depth of 5000 m. "Eta"–coordinate (Mesinger et al., 1985; Yu, 1989) is used to describe the complex bottom topography and the free surface of the ocean. A split time step is used in the temporal integration of the model (Mellor, 1993; Killworth et al., 1989,1991), and an implicit diffusion of the "upwind" advection scheme (Maier–Reimer et al., 1991) is adapted in temperature and salinity equations. Besides, a simple thermodynamic sea–ice model based on Semtner (1976) and Parkinson and Washington (1979) is incorporated. The model has been integrated over 1000 years with observed monthly mean atmospheric forcing, such as sea surface wind (Hellerman and Rosenstein, 1983) and temperature, water vapour

---

①The AMIP SST and Sea–ice Dataset was kindly provided by Program for Climate Model Diagnosis and Intercomparison (PCMDI), Lawrence Livermore National Laboratory.

mixing ratio, and etc, which were taken from Esbensen and Kushnir (1981). The model successfully simulates many major large–scale features of the world oceanic circulation, especially the thermohaline circulation.

In the current coupled model, the two component models interact with each other only through exchanges of anomalies of the heat and momentum, which are defined as the differences between the coupled and uncoupled states, that is,

$$F'_A = F_A(\Phi^b, \Psi^b, t) - F_A(\Phi^b_u, \Psi^b_u) \ ,$$
$$F'_O = F_O(\Phi^b, \Psi^b, t) - F_O(\Phi^b_u, \Psi^b_u) \ ,$$

where, F_A and F_O represent the fluxes of incoming into atmosphere and outgoing from the ocean respectively. The superscript "b" indicates the interface between the two subsystems, and the subscript "u" the equilibrium climates of the uncoupled models. The surface fresh water flux is computed as a function of the difference between climatologically prescribed surface skin salinity (Levitus, 1982) and the simulated surface–layer salinity rather than the difference between simulated evaporation and precipitation. The net downward surface heat flux over the ocean is calculated in terms of the Haney–type formula (Haney, 1971; Han, 1984; Zhang, R.–H., 1989). The "Prediction–Correction" Month mean anomaly coupling scheme (Zhang et al., 1992) is used to couple the atmosphere and ocean portions. That is, the flux anomaly exchange between the two components is carried out based on monthly mean atmospheric and oceanic variables of the coupled model, and the "prediction–correction" technique is used to decrease the effect due to the remarkable asynchronization of at least one component model with its "boundary" conditions provided by another component model. The procedure of the coupling scheme is as follows:

Step 1. The ocean model is integrated for one month with the current month "uncoupled climatological" fluxes (that is the fluxes computed from the uncoupled ocean model) plus "anomalous" fluxes averaged over the last month to find a guess solution to the prediction of the ocean (only climatological fluxes are used for the initial conditions of an integration). Hereafter, it is referred as "prediction step".

Step 2. The atmospheric model is then integrated for one month with current month "observed" SST plus monthly mean SST "anomaly" (the SST predicted in Step 1 minus that used in the uncoupled atmosphere model) to predict atmospheric state for the current month.

Step 3. The ocean model is re–integrated for the current month with the updated monthly mean flux "anomalies" obtained in Step 2 and the same "climatological" fluxes as used in Step 1 to get a corrected ocean state for the current month. Hereafter, it is referred as "correction step".

The coupling area is 46°N—58°S, that is, the ice free region in the model. The initial conditions for the coupled integration are taken as those simulated for 31 December of the year 11 of the uncoupled AGCM integration and year 1000 of the uncoupled OGCM integration. The uncoupled atmospheric variables are taken from the average of years 12— 14 of the AGCM integration with annual cycle and the uncoupled SST and sea ice are simply taken from year 1000 of the OGCM integration.

This CGCM has been integrated for 40 years and has shown only a little climate drifting. We will discuss this by means of the diagnoses of SST and sea–level air pressure (SLP) as well as the anomaly of downward heat flux into ocean.
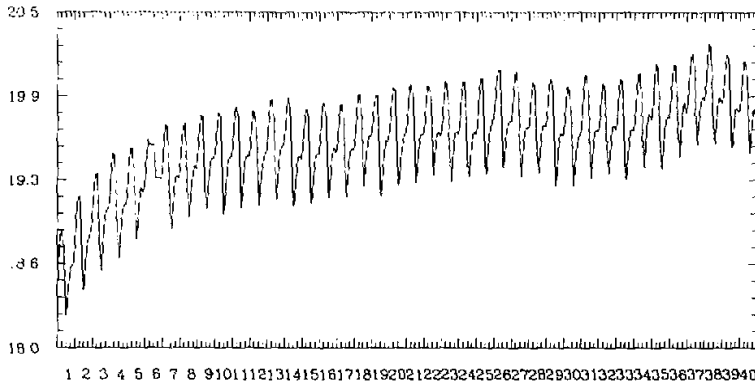
Fig. 1 The time evolution of monthly mean SST averaged over global ocean for the 40 years integration of the coupled model. unit: °C.
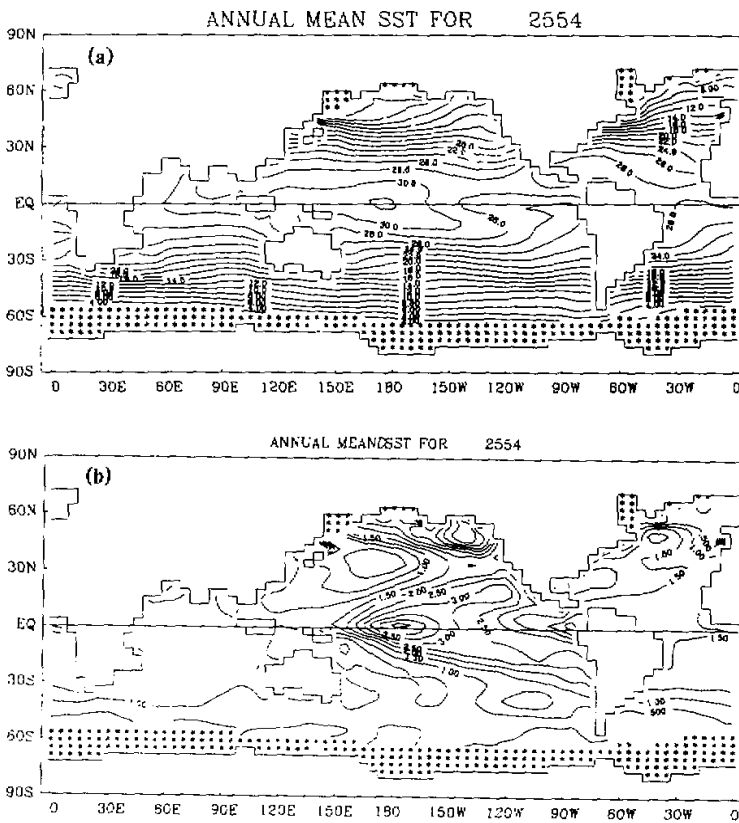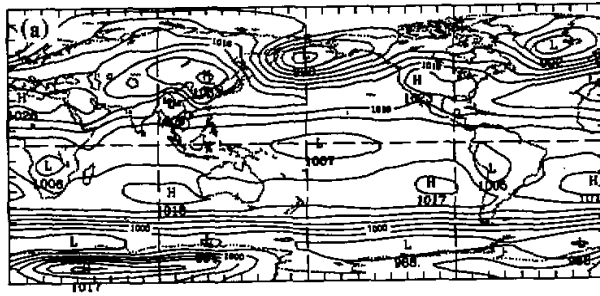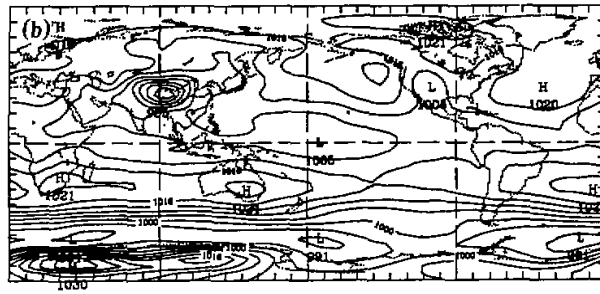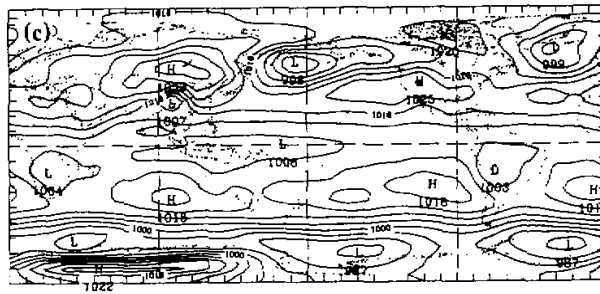

Fig. 2 (a) Global distribution of annual mean SST averaged for the last 30 years of the integration, (b) its deviation relative to the uncoupled SST from year 1000 of OGCM. units: °C.
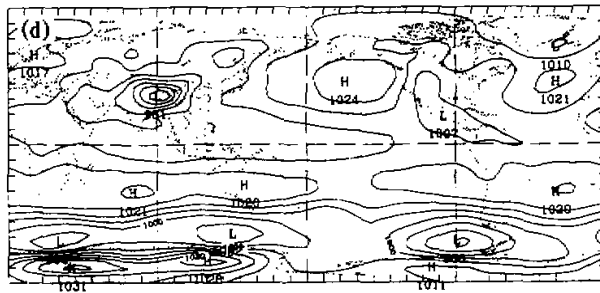
Fig. 3. Sea level air pressure (SLP) in (a), (b), coupled and (c), (d), uncoupled situation for January and July averaged for the last 20 years of the coupled integration. units: hPa.

III. THE SST, SLP AND OCEAN CURRENT FIELDS

The temporal evolution of the globally averaged monthly mean SST over the 40 years of the integration is shown in Fig. 1. One of the major features is that from the year 9 onward, the temperature does not increase much and possesses prominent fluctuations despite that the temperature increases rapidly during the first 8 years and about 0.7°C warmer than the uncoupled situation. The seasonal cycle is about 0.6°C, close to the corresponding one of the AMIP dataset.
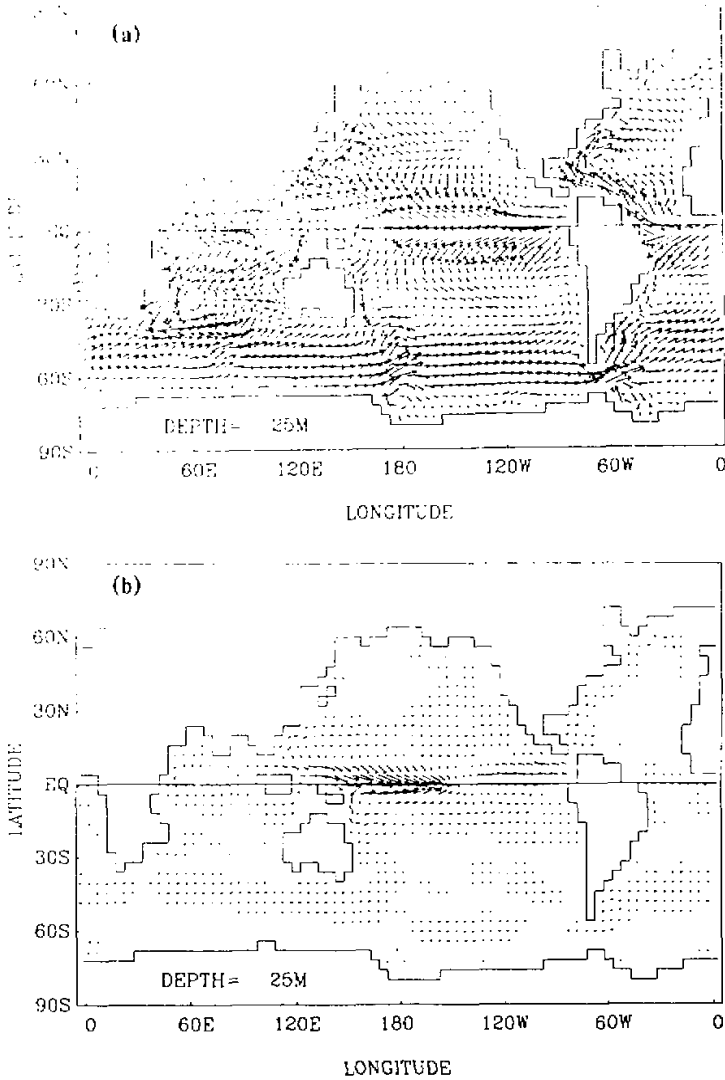

Fig. 4. (a) The simulated annual mean sea surface current which averaged over the last 30 years of the integration, (b) the current difference between the coupled and uncoupled ocean models.

Fig. 2 shows the annual mean SST averaged over the last 30—year and its derivation relative to the uncoupled one. The SST is about 4.5°C warmer in the western and northeastern Pacific, and about 2.0°C warmer in the northeastern Atlantic, but less than 1.0°C warmer in India ocean. However, an important feature is that the large—scale SST configuration of the warm pool in the western Pacific and the cold tongue in the east Pacific is still well kept.

Due to the changes of SST forcing, the sea—level air pressure in the coupled situation also has a few changes. In Fig. 3, the global distributions of January and July mean SLP climatology for the coupled and uncoupled situations are shown, the former is averaged for the last 20—year of the 40—year coupled integration and the latter for the last 3 year (that is, years 12—14) of the uncoupled integration. In January, the equatorial low in the western Pacific is about 1 hPa weaker than the uncoupled situation with its center shifted eastward, probably due to the increase of SST there. The Aleutian and Iceland lows are about 6 hPa and 7 hPa stronger respectively. The Siberian high has got the same strength as the uncoupled one but its position moves a little westward. The subtropical highs in the Southern Hemisphere are almost identical to the uncoupled ones. In July, subtropical highs in North Atlantic got little change in strength. The monsoon low remains at the same place as the uncoupled one but its intensity is about 4 hPa weaker. The subtropical highs in the Southern Hemisphere have little changes in their strength with a little movement in their position compared to the uncoupled situation.

Fig. 4a shows the simulated annual mean sea surface current which is averaged over the last 30 years of the integration. The equatorial easterly current, the "roaring forties", in the Southern Hemisphere, and the westward intensification of the circulation in the major ocean gyres are all well reproduced. The general features of the oceanic circulation system are in closely consistence with observation (Defant, 1961). However, the simulated off—east coast currents in the western oceans are relatively weak. This is in common with other models with coarse resolution. Fig.4b shows the current difference between the coupled and uncoupled ocean models. Remarkable weakening of the divergent equatorial current is found in the central Pacific. This will suppress the upwelling there and contribute to the increase of SST in the central equatorial Pacific. It accounts at least partly for the strong positive difference in SST in the central equatorial Pacific as shown in Fig. 2b.

IV. DOWNWARD SURFACE HEAT FLUX

It is accepted at the moment that the air and sea interact with each other mainly through exchanges of momentum, heat and fresh water. The last one is not considered in the current model. In this section, we focus on the heat exchange, especially the downward surface heat flux into or out of ocean. The heat flux at the prediction step will be analyzed. Its similarity with the heat flux at the correction step will be discussed later.

Let's first look at the observed heat flux (Fig. 5a) from Esbensen and Kushnir (1981), and the heat flux calculated from the year 1000 of the uncoupled OGCM integration (Fig. 5b), which is used as the climatological forcing of the current coupled OGCM. The two are quite similar but still have some differences. The dominant difference is that the maxima of heat flux into ocean in the far eastern Pacific in the observation are shifted much westward in the uncoupled integration. The heat flux out of ocean in high latitudes of the northern Atlantic and Pacific is weakened in the latter situation.

The time evolution of monthly mean heat flux anomaly averaged from 8°N to 8°S at the prediction step for the 40—year integration period is shown in Fig. 6. As mentioned before, this anomaly is defined as the difference between the heat flux at coupled situation and the

one at uncoupled situation. A major feature is that the heat flux anomaly is positive in the be-
ginning stage of the integration but the anomaly tends to fluctuate around zero in the last 10
years. From this, we are convinced that the coupled system is gradually reaching its equilibri-
um. Besides, a strong 10—year oscillation can be seen during the last 20 years.

The global distribution of the annual mean heat flux anomaly at the prediction step av-
eraged for the last 10 years is presented in Fig. 7. A strong upward heat flux anomaly out of
ocean is located in the central Pacific and a downward heat flux anomaly into ocean in the
eastern Pacific. This, to some extend, compensates the systematic errors of the uncoupled
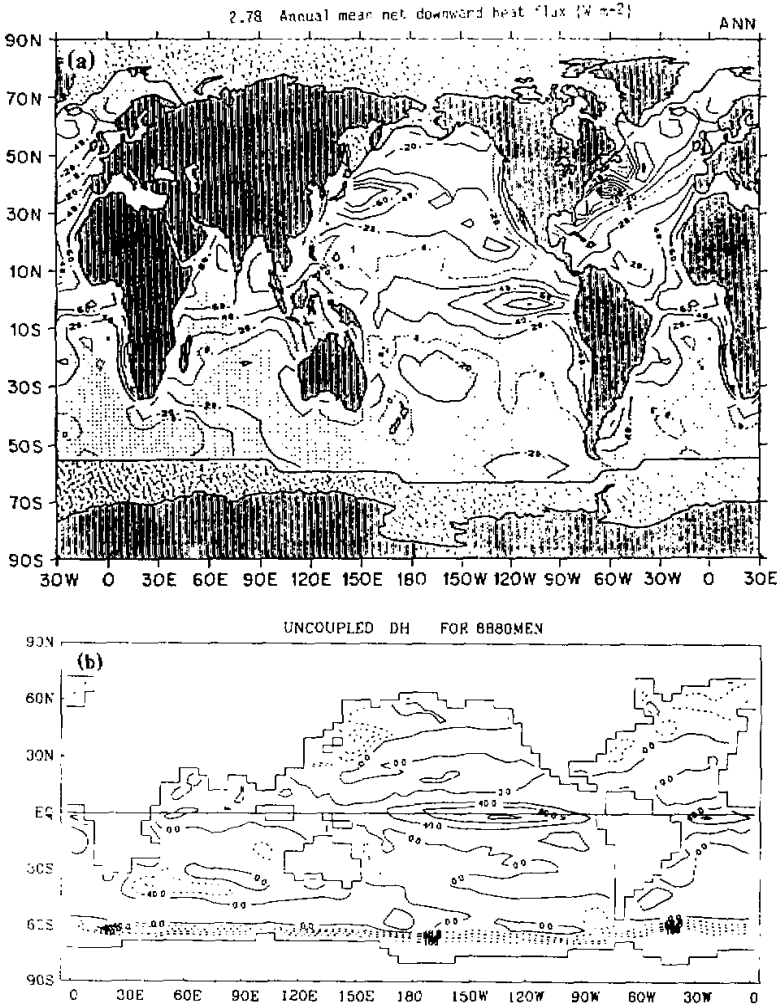OGCM as demonstrated by Fig. 5, and makes the total heat flux into the ocean there in the

Fig. 5. (a) The global distribution of observed annual mean heat flux, from Esbensen and Kushnir
(1982), and (b) the one calculated from year 1000 of uncoupled OGCM integration, positive for in-
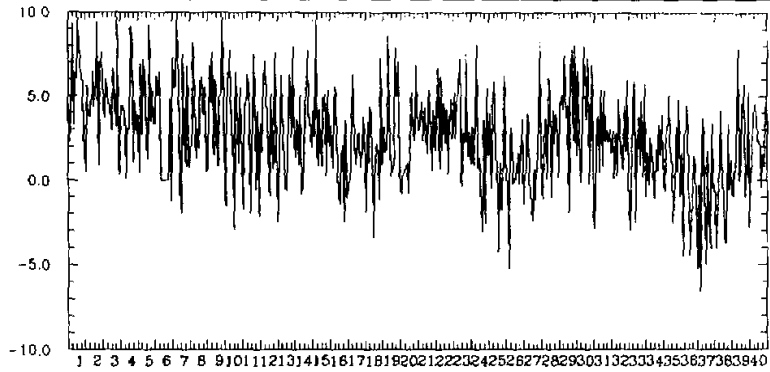to ocean. units: w / m².

Fig. 6. The time evolution of the monthly mean heat flux anomaly averaged from 8"N to 8"S at prediction step of the coupled ocean model for the 40-year integration. unit: w / m².
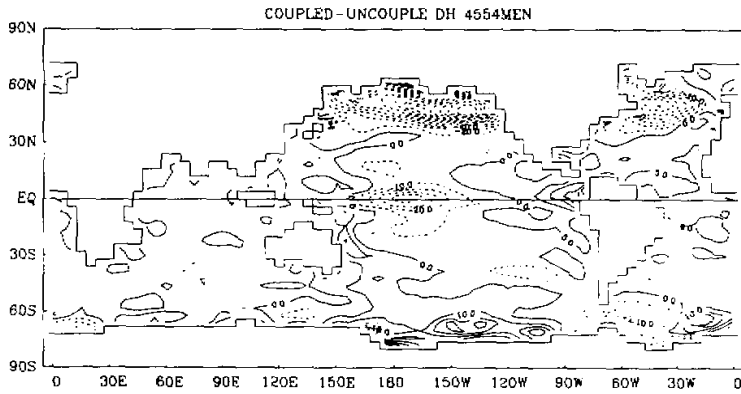
COUPLED-UNCOUPLE DH 4554MEN

Fig. 7. The global distribution of the annual mean heat flux anomalies at prediction step averaged for the last 10-years. unit: w / m².

LATITUDE
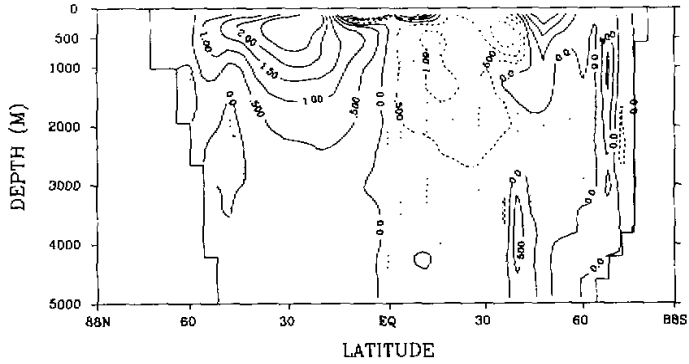
Fig. 8. The difference of the merdional thermohaline streamfunction which is averaged over global ocean between the averaged situation of the last 30 years of the coupled integration and year 1000 of the uncoupled integration. unit: Sv.

coupled situation closer to the observed one. Besides, in the north—eastern part of Pacific and Atlantic, the strong upward heat flux anomaly makes the total heat flux out of ocean much stronger than those in the uncoupled case, which is also closer to the observed one. Therefore, from the view point of heat flux, the coupled model still possesses some climate drifting, but seems to reach a more realistic state.

The thermohaline circulation of the ocean has corresponding changes to the heat flux anomalies. In Fig. 8, the difference of the meridional thermohaline stream function averaged over the global ocean between the one averaged for the last 30 years of the coupled integration and the year 1000 of the uncoupled integration is presented. A strong surface poleward flow derivation appears in the Northern Hemisphere, which transports the heat anomaly absorbed in equatorial region to the northern Pacific and Atlantic where at least part of the heat anomaly is out of the ocean. Another feature is that the interaction of the air—sea in the coupled case can reach the depth of about 2500 meters during the 40 years integration.

Finally in this section, the relation of the heat flux anomalies at the prediction and the correction steps is checked. The two items for annual mean case, averaged for the last 6 years, are shown in Fig. 9. They are almost identical. This suggests that the statistics from the heat flux anomalies at prediction step in annual mean situation can be used to represent the heat flux anomalies at the correction step. For monthly mean case, however, the two items differ a lot.
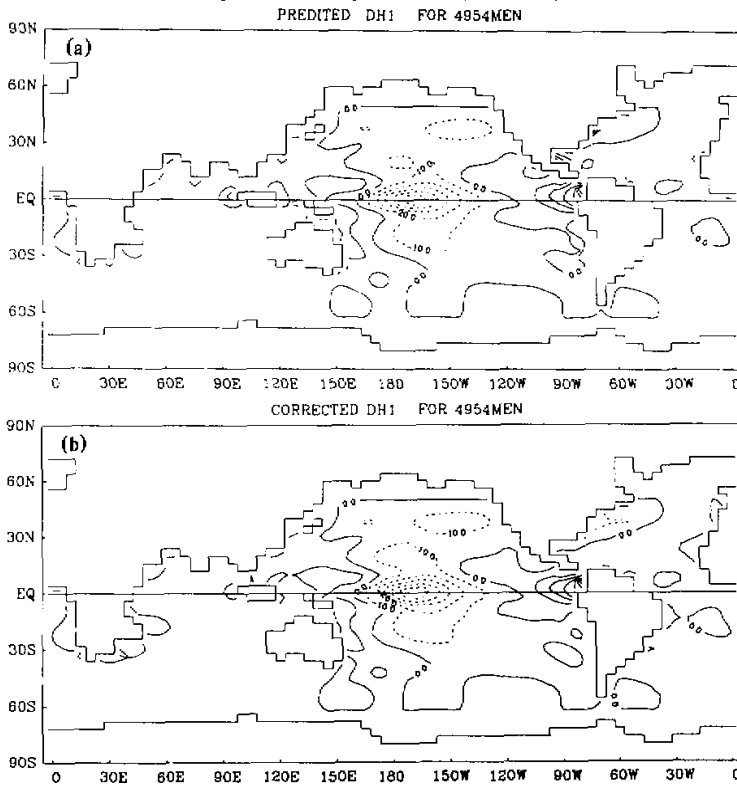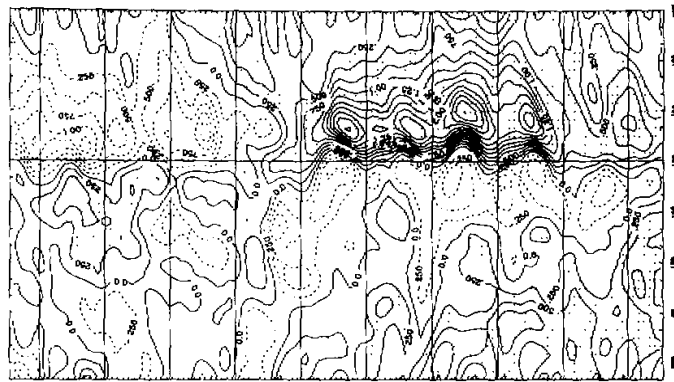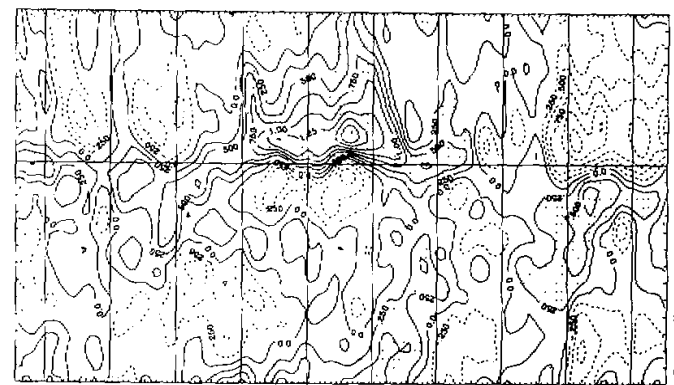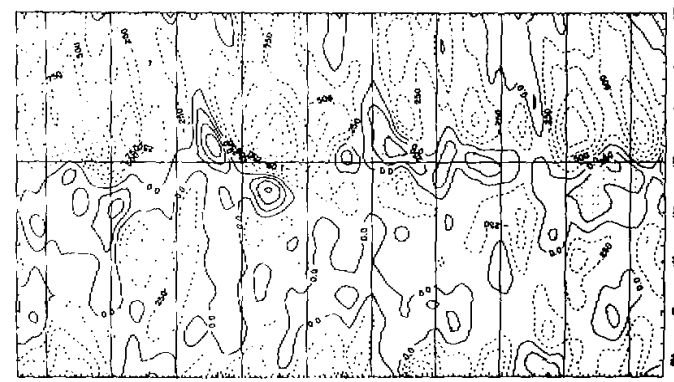

Fig. 9. the global distribution of heat flux anomalies at (a), the prediction step and (b), the correction step for annual mean case, which are the average of the last 6 years of the 40 year coupled integration. units: w / m^2.
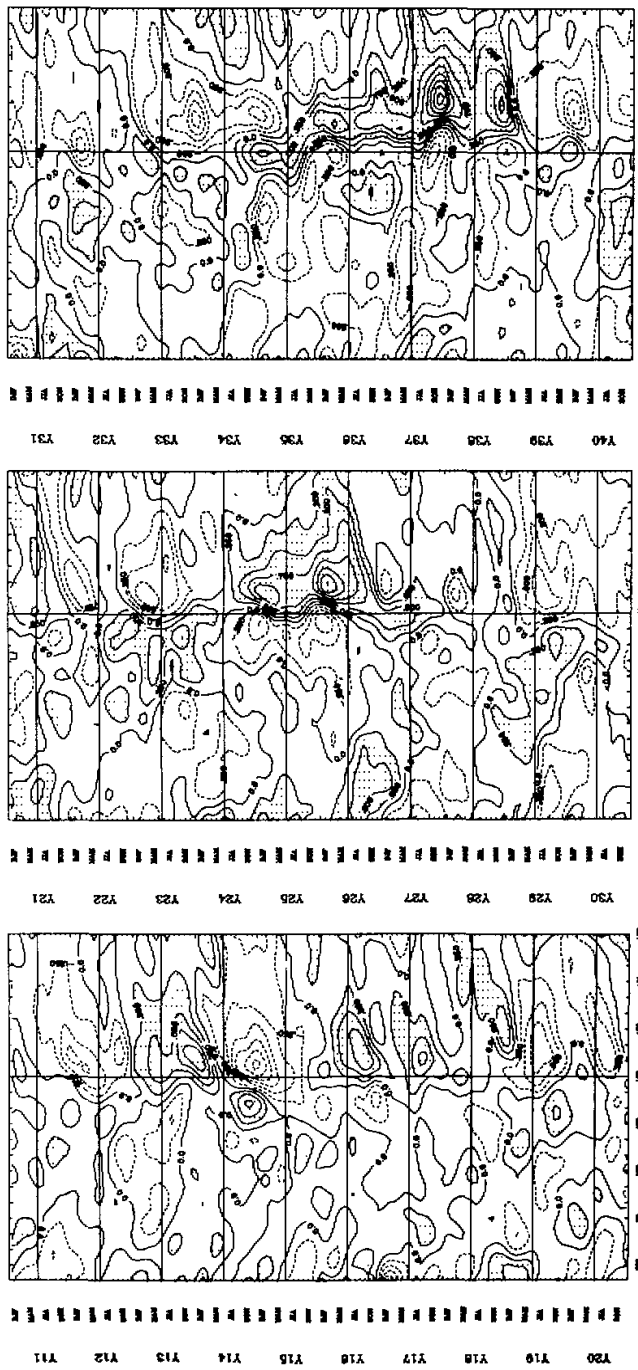
Fig. 10. The time–longitude plot of the simulated SST anomalies along the equatorial Pacific, averaged from 8°N to 8°S during the last 30 years of the coupled integration (relative to the mean value of the 30 years), unit; °C. (a) SST anomalies. (b) the SST anomalies in which the period longer than 7 years are removed.

V. INTERANNUAL VARIABILITY IN THE TROPICS

The time evolution of SST anomalies along the equatorial Pacific averaged from 8°N to 8°S for the last 30 years of the integration is presented in Fig. 10a. There are some implications of propagation of SST anomalies (westward and eastward) during a few years in the central and western Pacific, while in most years the SST anomalies tend to develop in places near the date—line. The frequency of the anomalies appears to become longer with time, from about 2—3 years to about 10 years. The magnitude of the anomalies also becomes stronger with time. The ENSO type anomalies are even more evident when anomalies of longer than 7 years are removed (Fig. 10b).

However, some remarkable systematic problems exist in Fig. 10. Most of the strong interannual variability appear near the dateline, while the signals in the eastern equatorial region are very weak. Furthermore, in the later stage of the simulation, the duration of the persistent SST anomaly for the same region is too long. They are far from reality and do not exist in the uncoupled OGCM. They may result from the coupling processes or from the imbalance of energy budget of the atmospheric column in the model. However, the exact reasons for these problems are still unclear, and further diagnoses and improvement are required.

VI. SUMMARY AND DISCUSSION

The CGCM is fairly successful in keeping a reasonable pattern of the modelled SST although most of the Pacific become warmer than those given by the uncoupled ocean model. The model tends to reach a more realistic state than the uncoupled ones in terms of downward surface heat flux into ocean, particularly in the equatorial Pacific region and sea—level air pressure. Also, the model has capability to produce interannual variability of sea surface temperature in tropical region. However, the intensity of this interannual variability is too weak, and its spatial and temporal evolutions are still far away from reality. As a whole, the results from the coupled GCM are encouraging, but still primary. Further efforts for its improvement are required.

REFERENCES

Defant, Albert (1961). Physical oceanography, Vol.1, Pergamon Press, 728 pp.

Esbensen, S.K. and Y. Kushnir (1981). Heat budget of the global ocean: estimates from surface marine observations. Report No.29, Climate research Institute, Oregon State Univ., Corvallis, Oregon, 271 pp.

Han, Y.—J. (1984). A numerical world oceanic general circulation model, Part 1: Basic design and barotropic experiment, Part 2: a baroclinic experiment. *Dynamics of Atmospheres and Oceans*. **8**: 107—172.

Haney, R.L. (1971). Surface thermal boundary condition for ocean circulation models, *J. Phys. Oceanogr.*, **1**: 241—248.

Hellerman, S. and Rosenstein, M. (1983). Normal monthly wind stress data over the world ocean with error estimates, *J. Phys. Oceanogr.*. **13**: 1093—1104.

Killworth, P.D., et al. (1989). A free surface Bryan—Cox—Semter model, Report No.270, Institute of Oceanographic Sciences, Deacon laboratory, 87 pp.

Killworth. P.D., et al. (1991). The development of a free surface Bryan—Cox—Semter model, *J. Phys. Oceanogr.*. **21**: 1333—1348.

Levitus, S. (1982). Climatological Atlas of the World Ocean, NOAA professional paper 13, US Government Printing Office, Washington, D.C., 173 pp.

Maier—Reimer, et al. (1991). On the sensitivity of the global ocean circulation to changes in the surface heat flux

forcing, Report 68, MPI, Hamburg, July, 1991, 67 pp.

Mellor, G.L. (1993),   User's guide for a three–dimensional, primitive equation, numerical ocean model, Princeton
   University, 35 pp.

Mesinger, F. and Janjic, Z.I. (1985),   Problems and numerical methods of the incorporation of mountains in atmos-
   pheric models, Lectures in Applied Mathematics, 22, 81–120.

Neelin, J.D., et al. (1992),   Tropical air–sea interaction in general circulation models, Climate Dynamics, 7: 73–104.

Parkinson, C.L., et al. (1979),   A large–scale numerical model of sea ice, J. Geophys. Res., 84: 311–337.

Sausen, R., et al. (1988),   Coupled ocean–atmosphere models with flux correction, Climate Dynamics, 2: 145–163.

Semtner, Jr. A. J. (1976),   A model for the thermodynamic growth of sea ice in numerical investigations of climate, J.
   Phys. Oceanogr., 6: 379–389.

Wu Guoxiong, Liu Hui, et al. (1996),   A nine–layer atmospheric general circulation Model and its performance, Ad-
   vances of Atmos. Sci.,13: 1–18.

Yu Rucong (1989),   Design of the limited area numerical weather prediction model with steep mountains, Scientia
   Atmospherica Sinica, 13: 139–149.

Zhang Ronghua (1989),   The numerical simulation studies for ocean circulation in the Pacific basin, Ph.D. thesis,
   Inst. of Atmos. Phys., Beijing.

Zhang X.–H., et al. (1992),   Coupling scheme experiments based on an atmospheric and an oceanic GCM, Chinese
   Journal of Atmospheric Sciences, 16(2) 129–144.

Zhang, X.–H., et al. (1994),   Simulation of thermohaline circulation with a twenty–layer oceanic general circulation
   model, Submitted to Theoretical and Applied Climatology.

Zeng Qingcun (1979),   Physical–mathematical basis of numerical weather prediction Vol. 1, Science Press, Beijing,
   543 pp. (in Chinese).